PNAS RESEARCH ARTICLE | NEUROSCIENCE OPEN ACCESS

Specific contribution of Reelin expressed by Cajal–Retzius cells or GABAergic interneurons to cortical lamination

Alba Vílchez-Acosta[a,b,1], Yasmina Manso[a,b,1], Adrián Cárdenas[c], Alba Elias-Tersa[a,b], Magdalena Martínez-Losa[d], Marta Pascual[a,b], Manuel Álvarez-Dolado[e], Angus C. Nairn[f], Víctor Borrell[c], and Eduardo Soriano[a,b,2]

Edited by Carol Mason, Columbia University, New York, NY; received November 3, 2021; accepted July 4, 2022

The extracellular protein Reelin, expressed by Cajal–Retzius (CR) cells at early stages of cortical development and at late stages by GABAergic interneurons, regulates radial migration and the "inside-out" pattern of positioning. Current models of Reelin functions in corticogenesis focus on early CR cell–derived Reelin in layer I. However, developmental disorders linked to Reelin deficits, such as schizophrenia and autism, are related to GABAergic interneuron–derived Reelin, although its role in migration has not been established. Here we selectively inactivated the *Reln* gene in CR cells or GABAergic interneurons. We show that CR cells have a major role in the inside-out order of migration, while CR and GABAergic cells sequentially cooperate to prevent invasion of cortical neurons into layer I. Furthermore, GABAergic cell–derived Reelin compensates some features of the *reeler* phenotype and is needed for the fine tuning of the layer-specific distribution of cortical neurons. In the hippocampus, the inactivation of Reelin in CR cells causes dramatic alterations in the dentate gyrus and mild defects in the hippocampus proper. These findings lead to a model in which both CR and GABAergic cell–derived Reelin cooperate to build the inside-out order of corticogenesis, which might provide a better understanding of the mechanisms involved in the pathogenesis of neuropsychiatric disorders linked to abnormal migration and Reelin deficits.

Cajal–Retzius cells | GABAergic interneurons | corticogenesis | neurodevelopmental disorders

Significance

The present study highlights a fundamental role of GABAergic interneuron-derived Reelin in neuronal migration, in addition to CR cell–expressed Reelin. Further, we observed transient migratory deficits, indicating that Reelin expressed by either neuronal population is sufficient to reverse some lamination defects. We propose a model of Reelin action in corticogenesis based on the spatial and cell-specific expression of this key protein. Because several neuropsychiatric disorders are linked to Reelin deficits in interneurons, this study may provide a better understanding of the mechanisms associated with human brain disorders related to Reelin deficits.

Correct lamination of the cerebral cortex is essential for normal brain function. In this regard, abnormal neuronal migration is common among many neurodevelopmental and neuropsychiatric disorders linked to cognitive impairment (1). Since the discovery that *Reln* is responsible for the *reeler* mutation (2), numerous studies support the idea that the extracellular protein Reelin is essential for neuronal migration and the layering of laminated structures, including the cerebral cortex and cerebellum (3–7). Inactivation of genes encoding for components of the Reelin pathway [e.g., the APOE2 and VLDL receptors (8), the adaptor Dab1 (9, 10), and the proteasome component Cullin-5 (11)] results in *reeler*-like phenotypes. These observations reinforce the relevance of this pathway for these developmental processes. This gene is also essential for the structural and functional organization of the blood–brain barrier (12).

In the developing cerebral cortex, Reelin is largely expressed by Cajal–Retzius (CR) cells, an early pioneer neuronal population, which, because of its strategic location in the marginal zone/layer I, Reelin secretion, morphogenetic-like functions, and transient nature, are considered essential in corticogenesis (13–15). Current models of Reelin action on migrating neurons, including Cadherin-mediated adhesion, Integrin-regulated detachment of radial glia, long-range and contact attraction/stop signaling, and Ephrin signaling, have mainly taken into consideration Reelin expressed by CR cells at the cortical surface (16–25). However, several studies report that CR cell ablation causes contradictory effects on corticogenesis (26–28). Reelin is also expressed by cortical GABAergic interneurons in the cortical plate (CP), long before the completion of cortical migration, persisting into adulthood (29). Recent studies have implicated Reelin in adult plasticity (30–33), as well as in the pathogenesis of neurodevelopmental, neuropsychiatric, and neurodegenerative diseases, notably in Alzheimer's disease, schizophrenia/bipolar disorder, autism spectrum disorder, and epilepsy (34–41), at stages when Reelin is mainly expressed by GABAergic neurons. Despite this, the contribution of Reelin expressed by GABAergic interneurons in cortical development is largely unknown and, consequently, the role of CR cell–derived Reelin might be overinterpreted. Only one recent study reports very mild migration deficits in the hippocampus of mice lacking Reelin in GABAergic interneurons (42).

Here we selectively inactivated the *Reln* gene in CR cells or GABAergic interneurons. We found both overlapping and specific functions of Reelin expressed by these two cell populations in distinct features of the *reeler* phenotype.

Author contributions: A.V.-A., Y.M., M.Á.-D., V.B., and E.S. designed research; A.V.-A., Y.M., A.C., A.E.-T., M.M.-L., M.P. and V.B. performed research; A.C.N. contributed new reagents/analytic tools; A.V.-A., Y.M., A.C., A.E.-T., M.P., V.B., and E.S. analyzed data; and A.V.-A., Y.M. and E.S. wrote the paper.

The authors declare no competing interest.

This article is a PNAS Direct Submission.

[1]A.V.-A. and Y.M. contributed equally to this work.

[2]To whom correspondence may be addressed. Email: esoriano@ub.edu.

This article contains supporting information online at http://www.pnas.org/lookup/suppl/doi:10.1073/pnas.2120079119/-/DCSupplemental.

Published September 6, 2022.

Results

Loss of Reelin from CR Cells Leads to Major Lamination Defects in the Neocortex. To study the role of Reelin expressed by specific neuronal populations, we generated a floxed *Reln* mouse line (*Reelin*$^{F/F}$), where the first exon is deleted upon Cre recombination. We validated the loss of Reelin in *Reelin*$^{F/F}$ mice upon expression of Cre recombinase by crossing this line with the ubiquitous inducible *Ubi-Cre*^{ERT2} mouse line. Tamoxifen treatment caused a complete loss of Reelin in Cre^{+} mice (*SI Appendix*, Fig. S1 *A*–*C*). Further, double *CR/GAD-Reelin*$^{F/F}$ mice (see below) showed a complete loss of Reelin expression and exhibited a cortical layering phenotype stronger than that in single mutants and reminiscent of the *reeler* phenotype, demonstrating that *Reln* inactivation in both CR and GAD^{+} neurons fully depletes cortical Reelin (*SI Appendix*, Fig. S1*F*). To determine the specific role of Reelin expressed by CR cells, we crossed the *Reelin*$^{F/F}$ mice with a line expressing Cre under the control of the Calretinin promoter [*CR-Reelin*$^{F/F}$ mice; *Calb2*$^{tm1(cre)Zjh}$/J] (*SI Appendix*, Fig. S1*D*). Homozygous *CR-Reelin*$^{F/F}$ mice survived well and did not exhibit any apparent abnormal motor behavior. Western blot (WB) analysis demonstrated a substantial decrease of Reelin in the cerebral cortex of *CR-Reelin*$^{F/F}$ mice from embryonic day 16 (E16) to postnatal day 1 (P1) and a slight reduction at P30, consistent with the transient presence of CR cells during embryonic cortical development (*SI Appendix*, Fig. S2*A*). To confirm the inactivation of *Reln* in CR cells, we performed immunohistochemistry (IHC) between E12 and E16 (Fig. 1 *A* and *B*), which revealed the absence of Reelin in cortical CR cells from E12 onwards in *CR-Reelin*$^{F/F}$ mice. To analyze the impact of CR cell–derived Reelin on cortical lamination, layer-specific Cux1 and CTIP2 antibodies were used. In control E16 embryos, CTIP2^{+} and Cux1^{+} neurons in the neocortex were concentrated mostly in different bands at the CP, with Cux1^{+} neurons being in the upper layers and CTIP2^{+} cells in the lower ones (Fig. 1*D*). In contrast, in *CR-Reelin*$^{F/F}$ embryos, Cux1^{+} neurons were distributed almost homogeneously through all cortical layers, and CTIP2^{+} neurons also had a wider distribution than in control littermates, including the upper layers (Fig. 1*E*). The two distinctive features of *CR-Reelin*$^{F/F}$ embryos were the remarkable invasion of Cux1^{+} neurons in the marginal zone (MZ) and the presence of both Cux1^{+} and CTIP2^{+} neurons (to a lesser extent) in the intermediate zone (IZ).

Analysis of Reelin expression at P1 further confirmed the absence of Reelin from CR cells and provided evidence for the presence of Calretinin^{-}/Reelin^{+} neurons, corresponding to GABAergic interneurons, scattered across the cortical layers, including layer I, in both mutant and control animals (Fig. 1*C*). Control animals showed two sharp, nonoverlapping bands labeled by Cux1 and CTIP2 antibodies within the CP (Fig. 1 *F* and *H*–*J*). However, in the neocortex of *CR-Reelin*$^{F/F}$ pups, Cux1^{+} and CTIP2^{+} neurons, despite being broadly separated in two main bands, showed a wider distribution than controls, intermingling with each other (Fig. 1 *G*–*J*). In addition, many Cux1^{+} and CTIP2^{+} neurons were located ectopically in lower layer VI and the IZ. Conversely, and coinciding with the expression of Reelin from GABAergic interneurons, the invasion of Cux1^{+} neurons into the MZ observed at E16 was no longer present at P1, suggesting a correction of this migration defect at perinatal stages.

At P30, Reelin^{+} interneurons in cortical layers were observed in both genotypes, including neurons in layer I. However, Reelin expression in the *CR-Reelin*$^{F/F}$ mice was absent in the subpopulation of Calretinin^{+} GABAergic interneurons, which account for about 4 to 6% of Reelin^{+} cortical interneurons (43). This observation thus further validates the specificity of the *CR-Reelin*$^{F/F}$ mouse line for Calretinin^{+} cells (*SI Appendix*, Fig. S2 *B* and *C*). The abnormal distribution of cortical neurons in *CR-Reelin*$^{F/F}$ mice described at earlier stages persisted throughout maturation. Whereas in control mice Cux1 and CTIP2 expression defined two bands of cells, corresponding to layers II–IV and V–VI, respectively, this pattern was significantly altered in *CR-Reelin*$^{F/F}$ mice. Substantial numbers of Cux1^{+} neurons continued to be located ectopically in deep layers, and CTIP2^{+} neurons concentrated narrowly in layer V and upper layer VI. Similar to P1, layer I in *CR-Reelin*$^{F/F}$ mice was devoid of ectopic Cux1+ neurons at P30 (Fig. 2 *A*–*C*).

To determine whether the mispositioning of Cux1^{+} and CTIP2^{+} cells was due to defects in cell migration or molecular identity, we performed 5-Bromodeoxyuridine (BrdU)-birthdating studies. Neurons were labeled with BrdU at E12 or E15, and their final location was assessed at P30 (Fig. 2 *D*–*G*). In control mice, E12-labeled neurons occupied layers V-VI, and E15-labeled neurons were found in layers II–III. In *CR-Reelin*$^{F/F}$ mice, E12-born neuron distribution was similar to controls, whereas many E15-born neurons were located ectopically in layers V–VI. Together, these findings indicate that the lack of Reelin in CR cells leads to the permanent mispositioning of cortical neurons, with a large number of upper layer–fated neurons located in deep layers. The absence of CR cell–derived Reelin also caused a transient mislocation of Cux1^{+} neurons in layer I at E16, which was corrected at later stages.

Loss of Reelin from GABAergic Interneurons Leads to Permanent Neuronal Ectopias in Layer I. To study the role of Reelin expressed by GABAergic interneurons, we crossed *Reelin*$^{F/F}$ mice with *Gad2*$^{tm2(cre)Zjh}$/J counterparts expressing Cre under the control of the Gad2 promoter (*GAD-Reelin*$^{F/F}$ mice) (*SI Appendix*, Fig. S1*E*). *GAD-Reelin*$^{F/F}$ mice survived well and showed no signs of abnormal motor behavior. WB analysis confirmed a reduction of Reelin protein in *GAD-Reelin*$^{F/F}$ mice, which was conspicuous at P30 (*SI Appendix*, Fig. S3*A*). *GAD-Reelin*$^{F/F}$ embryos showed normal expression of Reelin in CR cells at E16, before the onset of Reelin expression in GAD^{+} neurons (*SI Appendix*, Fig. S3*B*). No differences were found in the distribution of Cux1^{+} and CTIP2^{+} neurons between control and *GAD-Reelin*$^{F/F}$ embryos at E16, with Cux1^{+} neurons being correctly positioned in the upper CP and CTIP2^{+} neurons in the deepest region of the CP (Fig. 3*A*).

At P1, Reelin expression by CR cells persisted in both genotypes, but while control mice exhibited scattered Reelin^{+} neurons in the CP corresponding to GABAergic interneurons, the expression of this protein in these layers was absent in *GAD-Reelin*$^{F/F}$ mice (*SI Appendix*, Fig. S3*C*). These expression data agree with studies reporting that Reelin is already expressed in CP GABAergic neurons by E17–E18, whereas in the MZ, Reelin is exclusively expressed by CR cells at E12–E19, with expression starting in layer I interneurons by P0–P1 (18, 29).

The distribution of Cux1^{+} and CTIP2^{+} neurons into two separate layers was evident in both genotypes at this stage. However, we already noted a few Cux1^{+} neurons located ectopically in layer I in *GAD-Reelin*$^{F/F}$ mice and accumulation of these neurons at the top of layer II (Fig. 3 *B*–*E*). At later developmental stages (P30), Reelin was expressed in GABAergic interneurons and was widely distributed throughout cortical layers, including layer I in control mice. In contrast, the cortex of *GAD-Reelin*$^{F/F}$ mice was virtually devoid of Reelin expression (*SI Appendix*, Fig. S3 *D* and *E*). The distribution of Cux1^{+} and

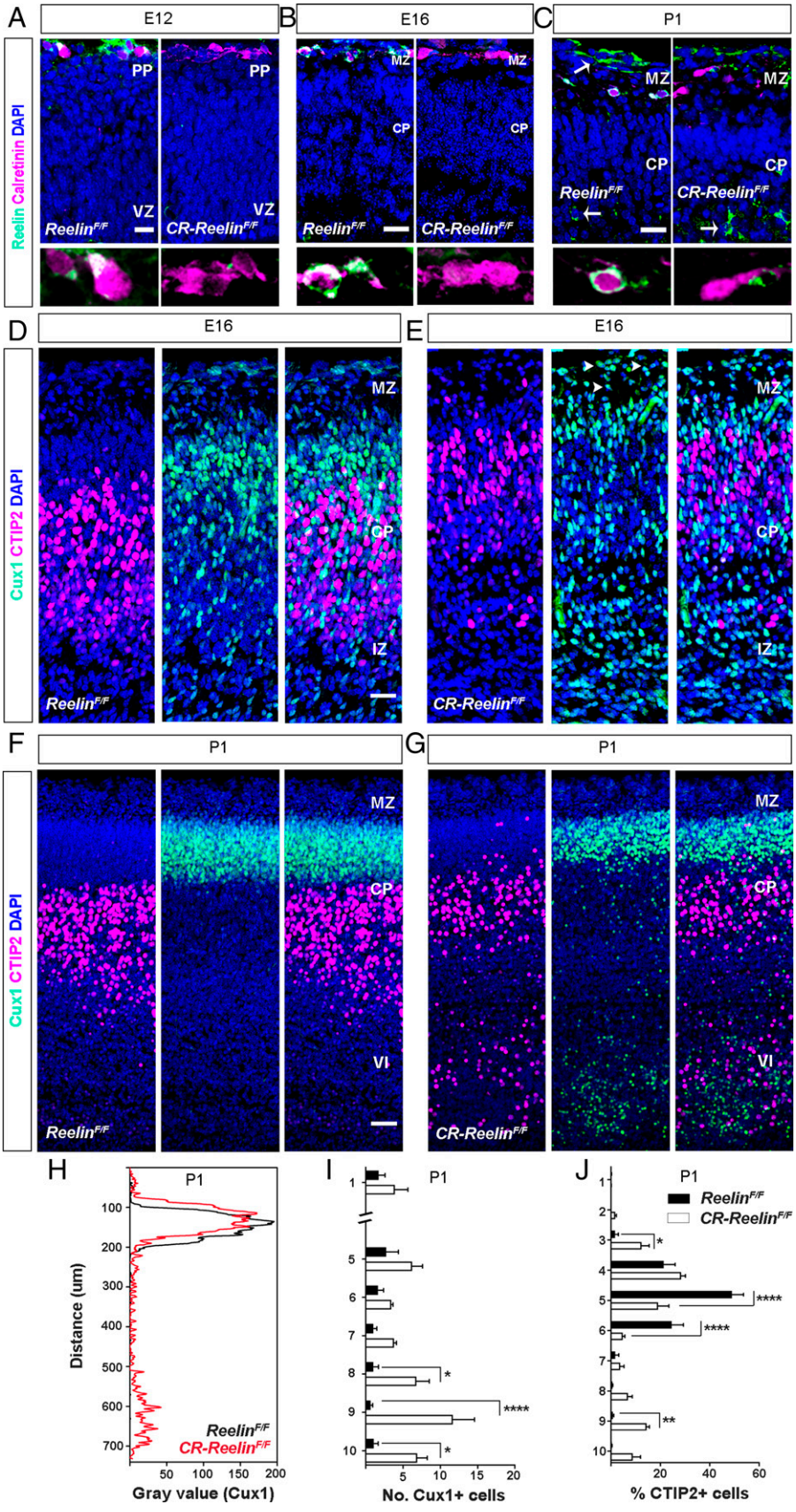

Fig. 1. Cortical neuronal distribution at E16 and P1 in the absence of Reelin from CR cells. (*A–C*) Double IHC of Reelin$^+$ (green) and Calretinin$^+$ cells (magenta) at E12 (*A*) E16 (*B*), and P1 (*C*) in the presence (*Reelin$^{F/F}$*, *Left*) and absence (*CR-Reelin$^{F/F}$*, *Right*) of Reelin from CR cells. Magnification of MZ cells (*A*, *B*, *C*, *Bottom*). Note the colocalization of Reelin and Calretinin staining in the *Reelin$^{F/F}$* but not in the *CR-Reelin$^{F/F}$* brain. Reelin$^+$ interneurons start to be present in the *Reelin$^{F/F}$* and the *CR-Reelin$^{F/F}$* cortices, including the CP and MZ, from P1 onwards (arrows). (*D* and *E*) Confocal images depicting the cortical distribution of Cux1$^+$ (green, upper layers) and CTIP2$^+$ cells (magenta, lower layers) at E16 in the presence (*Reelin$^{F/F}$*; *D*) and absence of Reelin from CR cells (*CR-Reelin$^{F/F}$*; *E*). Note the presence of Cux1$^+$ cells located ectopically in the MZ (arrowheads) and the wider distribution of Cux1$^+$ and to a lesser extent CTIP2$^+$ cells throughout the cortical layers in the *CR-Reelin$^{F/F}$* but not in the *Reelin$^{F/F}$* mice. (*F* and *G*) Cortical distribution of Cux1$^+$ and CTIP2$^+$ cells at P1 in *Reelin$^{F/F}$* (*F*) and *CR-Reelin$^{F/F}$* (*G*) mice evidencing clusters of ectopic Cux1$^+$ and CTIP2$^+$ cells in lower layer VI and the IZ of *CR-Reelin$^{F/F}$* mice. (*H*) Representative profile of Cux1 intensity (gray value) over distance (from MZ to layer VI) in P1 *Reelin$^{F/F}$* (black) and *CR-Reelin$^{F/F}$* (red) mice. (*I*) Quantification of the number of Cux1$^+$ cells per bin at P1. Note the absence of ectopic Cux1$^+$ cells in the MZ at this stage in *CR-Reelin$^{F/F}$* mice. (*J*) Quantification of the percentage of CTIP2$^+$ cells per bin at P1. Data represent mean ± SEM. Statistical analysis: (*I*) bin × genotype interaction $F(6, 42) = 3.108$ $P = 0.0131$; two-way ANOVA with Bonferroni post hoc test; $^*P < 0.05$, $^{****}P < 0.0001$, $n = 4$ mice per genotype. (*J*) Bin × genotype interaction $F(9, 60) = 16.54$ $P < 0.0001$; two-way ANOVA with Bonferroni post hoc test; $^*P < 0.05$, $^{**}P < 0.01$, $^{****}P < 0.0001$, $n = 4$ mice per genotype. (Scale bar in *A*, 15 μm; *B* and *C*, 20 μm; *D* and *E*, 25 μm; and *F* and *G*, 50 μm.) Pre-plate (PP), Ventricular Zone (VZ), Marginal zone (MZ), cortical plate (CP), intermediate zone (IZ), and layer VI (VI).

CTIP2$^+$ neurons in the upper and lower cortical layers, respectively, differed slightly in the two genotypes, with Cux1$^+$ cells scattered in lower cortical layers of *GAD-Reelin$^{F/F}$* mice (Fig. 3 *F–H*). Remarkably, at both P15 and P30, there was a massive invasion of ectopic Cux1$^+$ neurons in layer I of *GAD-Reelin$^{F/F}$* mice (Fig. 3 *F* and *I*). To substantiate these defects, E12 and E15 embryos were pulse labeled with BrdU and analyzed at P30. The distribution of E12-born neurons was similar between

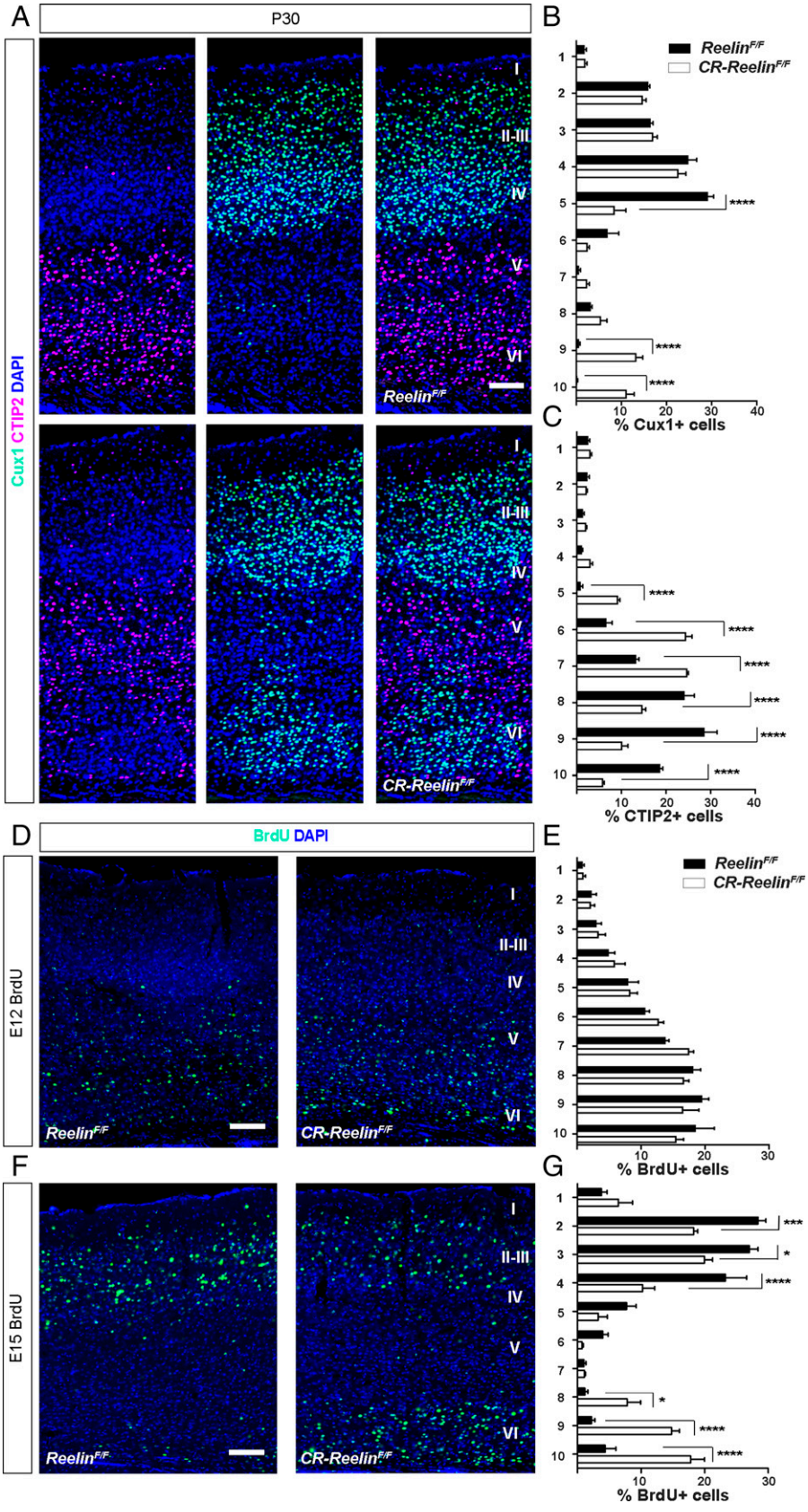

Fig. 2. Cortical neuronal distribution at P30 in the absence of Reelin from CR cells. (*A*) Confocal images at P30 illustrating the cortical distribution of Cux1$^+$ (green, upper layers) and CTIP2$^+$ cells (magenta, lower layers) in *Reelin$^{F/F}$* (*Top*) and *CR-Reelin$^{F/F}$* mice (*Bottom*). (*B* and *C*) Quantification of the percentage of Cux1$^+$ (*B*) and CTIP2$^+$ (*C*) cells per bin at P30 confirming the persistence of ectopic clusters of Cux1$^+$ cells in the lower layers of *CR-Reelin$^{F/F}$* mice. Note the absence of ectopic Cux1$^+$ cells invading layer I also at this stage. (*D* and *F*) BrdU immunohistochemistry of P30 mice injected with BrdU at E12 (*D*) and E15 (*F*). (*E* and *G*) Quantification of the percentage of BrdU$^+$ cells per bin in mice injected either at E12 (*E*) or E15 (*G*), further demonstrating the lamination abnormalities in *CR-Reelin$^{F/F}$* mice. Data represent mean ± SEM. Statistical analysis: (*B*) bin × genotype interaction $F(9, 60) = 29.96$ $P < 0.0001$; two-way ANOVA with Bonferroni post hoc test; ****$P < 0.0001$, $n = 4$ mice per genotype. (*C*) Bin × genotype interaction $F(9, 60) = 64.53$ $P < 0.0001$; two-way ANOVA with Bonferroni post hoc test; ****$P < 0.0001$, $n = 4$ mice per genotype. (*E*) Bin × genotype interaction $F(9, 60) = 1.503$ $P = 0.1677$ n.s.; $n = 4$ mice per genotype. (*G*) Bin × genotype interaction $F(9, 60) = 18.29$ $P < 0.0001$; two-way ANOVA with Bonferroni post hoc test; *$P < 0.05$, ***$P < 0.001$, ****$P < 0.0001$, $n = 4$ mice per genotype. (Scale bar, 100 μm.) Cortical layer in roman numerals.

control and *GAD-Reelin$^{F/F}$* mice, with most BrdU$^+$ cells in layers V and VI. In contrast, E15-born neurons, which in control mice were concentrated mostly in layers II–III, were found ectopically invading layers I and VI in *GAD-Reelin$^{F/F}$* mice (*SI Appendix*, Fig. S4 *A–D*). Double staining of BrdU with Cux1 confirmed that in *GAD-Reelin$^{F/F}$* mice most Cux1$^+$ neurons ectopically located either in layer I or VI were born at E15, and hence destined to layers II–III (Fig. 3 *J* and *K*). These findings suggest that expression of Reelin by GABAergic interneurons is largely dispensable for early cortical migration and the overall

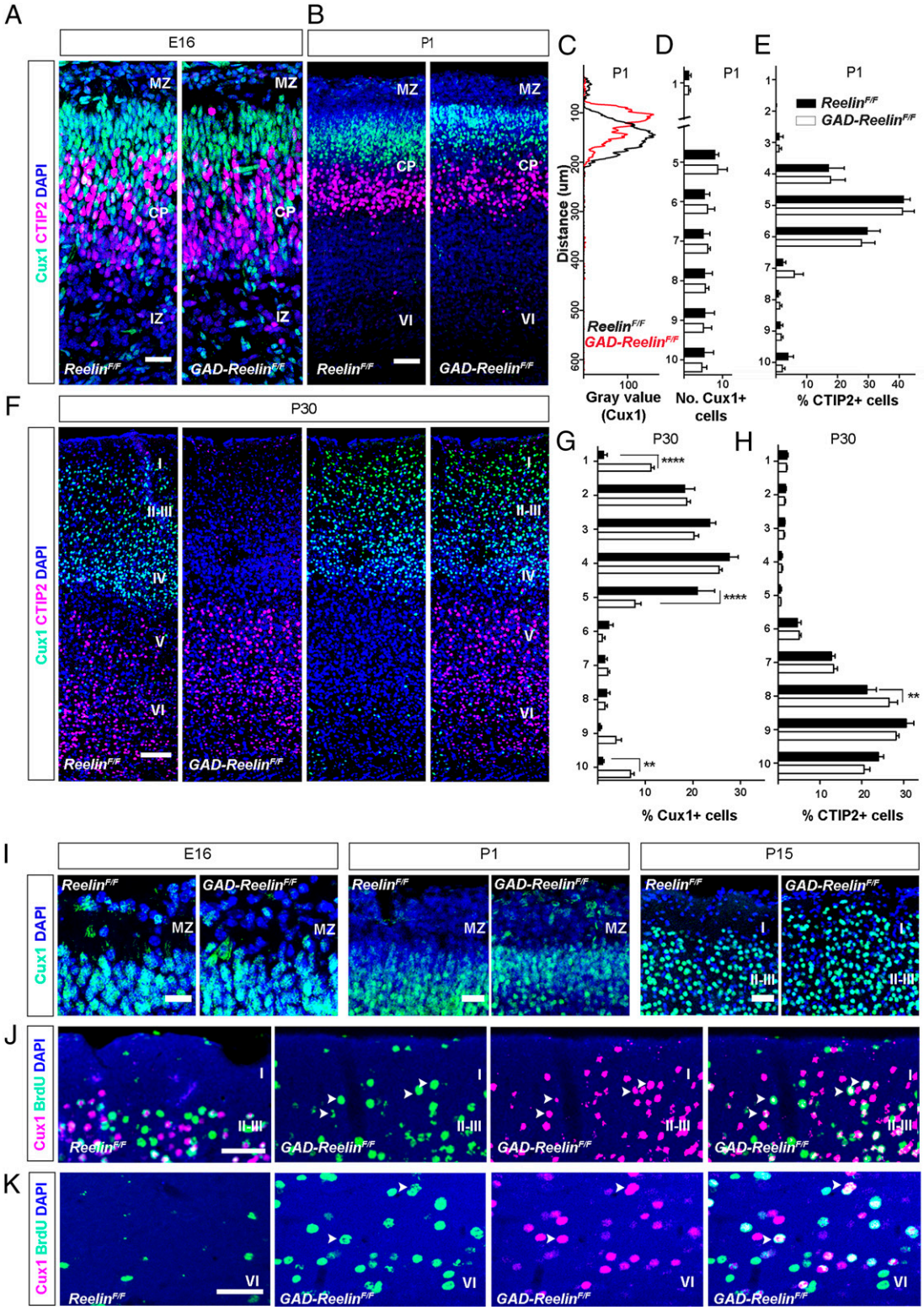

Fig. 3. Distribution of cortical neurons in the absence of Reelin from GABAergic interneurons. (*A*, *B*, and *F*) Confocal images showing the cortical distribution of Cux1$^+$ (green, upper layers) and CTIP2$^+$ cells (magenta, lower layers) in *Reelin$^{F/F}$* (*Left*) and *GAD-Reelin$^{F/F}$* (*Right*) at E16 (*A*), P1 (*B*), and P30 (*F*). (*C*) Representative profile of Cux1 intensity (gray value) over distance (from MZ to layer VI) in P1 *Reelin$^{F/F}$* (black) and *GAD-Reelin$^{F/F}$* (red) mice. (*D* and *E*) Quantification of the number of Cux1$^+$ (*D*) and the percentage of CTIP2$^+$ (*E*) cells per bin at P1. (*G* and *H*) Quantification of the percentage of Cux1$^+$ (*G*) and CTIP2$^+$ (*H*) cells per bin at P30. (*I*) Cux1 IHC illustrating the time course of layer I invasion in *GAD-Reelin$^{F/F}$* mice. Note that at embryonic stages, when CR cells are the main source of Reelin, *Reelin$^{F/F}$* and *GAD-Reelin$^{F/F}$* mice are virtually indistinguishable. Notably, at later stages Cux1$^+$ cells start to ectopically accumulate at lower cortical layers and at the top of layer II and to progressively and massively invade layer I. (*J* and *K*) Double staining of BrdU$^+$ (green) and Cux1$^+$ cells (magenta) from P30 mice injected with BrdU at E15, (*J*) layer I, and (*K*) layer VI. Arrowheads indicate double-labeled cells. Data represent mean ± SEM. Statistical analysis: (*D*) bin $F(6, 35) = 3.373$ $P = 0.0099$; two-way ANOVA with Bonferroni post hoc test; n.s., nonsignificant; *Reelin$^{F/F}$* $n = 4$; and *GAD-Reelin$^{F/F}$* $n = 3$. (*E*) Bin × genotype interaction $F(9, 50) = 0.2055$ $P = 0.9924$, n.s.; *Reelin$^{F/F}$* $n = 4$ and *GAD-Reelin$^{F/F}$* $n = 3$. (*G*) Bin × genotype interaction $F(9, 80) = 13.9$ $P < 0.0001$; two-way ANOVA with Bonferroni post hoc test; $^{**}P < 0.01$, $^{****}P < 0.0001$, $n = 5$ mice per genotype. (*H*) Bin × genotype interaction $F(9, 70) = 2.717$ $P = 0.0089$; two-way ANOVA with Bonferroni post hoc test; $^{**}P < 0.01$, *Reelin$^{F/F}$* $n = 4$ and *GAD-Reelin$^{F/F}$* $n = 5$. (Scale bar in *A*, 25 μm; *B*, *J*, and *K*, 50 μm; *F*, 100 μm; *I*, 15 μm for E16; 25 μm for P1, and 50 μm for P15.)

formation of layers, as long as Reelin is supplied by CR cells. However, at later stages, the absence of GABAergic interneuron–derived Reelin allowed the ectopic invasion of layer I by Cux1$^+$ neurons otherwise fated for layers II–III. Further, the lack of GABAergic interneuron–derived Reelin resulted in the appearance of ectopic layer II–III neurons in deep layers and in subtle laminar alterations in the remaining layers.

Reelin from Interneurons Is Sufficient for the Gross Formation of CA1 in the Absence of Reelin from CR Cells. We next examined cell-specific Reelin inactivation in another key layered structure, the hippocampus. In contrast to the neocortex, Reelin expression in the hippocampus persists in some CR cells through adulthood (44) and coexists with the expression of this protein by GABAergic interneurons. At E16/P1, hippocampal CR cells identified by Calretinin immunostaining coexpressed Reelin in control samples. Reelin$^+$ CR cells were densely packed at the stratum lacunosum-moleculare/molecular layer (SLM/ML) interphase, near the hippocampal fissure. In *CR-Reelin*$^{F/F}$ animals, the dense band of Reelin$^+$ CR cells located at the SLM/ML interphase were absent, whereas Reelin expression persisted in presumed GABAergic neurons (*SI Appendix*, Fig. S5*A*). The general organization of the hippocampal fields of control and *CR-Reelin*$^{F/F}$ mice appeared to be similar, with the main subdivisions being recognizable (*SI Appendix*, Fig. S6). However, at P1, the cornu ammonis (CA)1 pyramidal layer (PL) tended to be thicker in the latter (*Reelin*$^{F/F}$: 90.48 ± 0.71 μm; *CR-Reelin*$^{F/F}$: 113 ± 14.83 μm, $P = 0.1347$ t = 2.035 df = 3), and the sharp border with the stratum radiatum (SR) was irregular and discontinuous in mutant mice, suggesting migration abnormalities (Fig. 4*A*). At P30 in control mice, Reelin was expressed by the remnants of hippocampal CR cells in the SLM/ML and by a large number of GABAergic neurons in the different layers of the hippocampus. In *CR-Reelin*$^{F/F}$ mice, Reelin expression was absent specifically in CR cells, while it was widely expressed in GABAergic neurons (*SI Appendix*, Fig. S5*B*). Calretinin$^+$/Reelin$^+$ interneurons accounted for only about 3% of Reelin$^+$ interneurons. As at previous ages, the PL was slightly thicker in *CR-Reelin*$^{F/F}$ mice compared to controls and the sharp border between this layer and the SR was disturbed in *CR-Reelin*$^{F/F}$ mice, with ectopic pyramidal neurons in the SR (Fig. 4 *B–D*). To analyze migratory deficits in the pyramidal neurons, we performed analyses of BrdU pulse labeling at E12 and E15. At both ages, pyramidal neurons in *CR-Reelin*$^{F/F}$ mice tended to display a wider distribution within the PL than controls (Fig. 4 *E* and *F*). Taken together, our results suggest that Reelin from interneurons is sufficient for the gross formation of layers in CA1.

We next examined the CA1 region of *GAD-Reelin*$^{F/F}$ mutant embryos and postnatal mice, which exhibited strong Reelin expression around the SLM/ML interphase, corresponding to CR cells. In contrast, in these mutants, Reelin expression was absent from hippocampal GABAergic interneurons, which were scattered across the different layers (*SI Appendix*, Fig. S7 *A* and *B*). Of note, the CA1 laminar organization and inside-out migration pattern were not altered in this model, as evidenced by BrdU-birthdating studies (*SI Appendix*, Fig. S8 *A*, *B*, *E*, and *F*). We thus conclude that the expression of Reelin by either CR cells or GABAergic interneurons in the hippocampus proper is sufficient to maintain the laminar organization in this region, with minor alterations in the PL.

Lack of Reelin in CR Cells Results in Dramatic Anatomical and Migration Alterations in the Dentate Gyrus. We next studied the lamination and migration pattern of the dentate gyrus (DG), a region with long-lasting postnatal neurogenesis. As described above, both Reelin$^+$ CR cells and GABAergic neurons coexisted at the SLM/ML interphase at E16/P1 stages. Reelin was absent in CR cells in *CR-Reelin*$^{F/F}$ mice (*SI Appendix*, Fig. S5). Interestingly, at E16/P1, the emerging granule layer (GL) in the DG of *CR-Reelin*$^{F/F}$ mutants was less delineated, with widespread distribution of granule cells (GCs) in the hilus, in contrast to the densely packed GL of controls (Fig. 5*A*). At P15/P30, the DG of *CR-Reelin*$^{F/F}$ mice showed severe abnormalities. First, the GL was considerably thicker in these mutants, often showing accumulation of GCs in large patches that ectopically invaded the ML. Second, most *CR-Reelin*$^{F/F}$ mice (12 of 18) virtually lacked an infrapyramidal blade in the DG, or it was extremely short (<350 μm; 2 of 18 animals) (Fig. 5 *B–D*). BrdU pulses at E15 or P10–11 revealed the widespread laminar distribution of GC in the DG of *CR-Reelin*$^{F/F}$ mice (Fig. 5 *E* and *F*). In contrast, the laminar organization and outside-in migration pattern in the *GAD-Reelin*$^{F/F}$ mice, which have Reelin expression in large numbers of surviving CR cells, remained unaltered throughout development (*SI Appendix*, Figs. S7 and S8 *C*, *D*, *G*, and *H*). Together, these findings suggest that the lack of Reelin expression by hippocampal CR cells results in morphogenetic malformations and aberrant migration in the DG and that GABAergic neuron–derived Reelin is largely dispensable for the correct layering of the DG when Reelin expressed by CR cells is present.

Reelin Inactivation in CR Cells Leads to *reeler*-Like Morphological Phenotypes. To substantiate the above findings, we performed "in utero" electroporation experiments in which DNA encoding GFP under the ubiquitous CAG promoter was electroporated at E14.5 in the ventricle of control *Reelin*$^{F/F}$ and mutant *CR-Reelin*$^{F/F}$ embryos, and labeled cells were analyzed at P1. In control embryos, GFP-labeled neurons were concentrated in the upper CP (layers II–III). In contrast, in *CR-Reelin*$^{F/F}$ mutants, fewer GFP$^+$ neurons reached the CP and were also located ectopically in deep layers (Fig. 6 *A* and *B*). In addition, GFP$^+$ cells displayed marked morphological alterations. In control animals, most GFP$^+$ neurons exhibited typical pearl-to-pyramidal shapes and a prominent, radially oriented apical process, perpendicular to the MZ (Fig. 6*C*). The apical process of most GFP$^+$ neurons in *CR-Reelin*$^{F/F}$ mice showed an oblique or horizontal orientation, parallel to the MZ (Fig. 6*D* and *SI Appendix*, Fig. S9*A*). Moreover, GFP$^+$ neurons located in deep layers lacked an obvious apical dendrite but had round cell bodies and exhibited stellate-like morphologies (Fig. 6*E*). These altered morphologies are largely reminiscent of those found in *reeler* mice and *Dab1* knockout mice (20, 45). Thus, the lack of Reelin expression in CR cells is sufficient to render a *reeler*-like phenotype in layer II–III neurons.

Postnatal Expression of Reelin in *GAD-Reelin*$^{F/F}$ Mice Reduces Layer I Invasion. E14.5 *CR-Reelin*$^{F/F}$ electroporated embryos were also analyzed at earlier stages (E18–E19). We found occasional GFP$^+$ neurons in the MZ/CP interphase displaying leading-like processes with horizontal or even basal orientation, which may be compatible with an inward migration (*SI Appendix*, Fig. S9*B*), suggesting that at least some ectopic neurons in the MZ at E16 (Fig. 1*E*) might undergo inward migration at perinatal stages.

Next, we grafted E13.5 GFP-tagged GABAergic cell precursors (medial ganglionic eminence [MGE]) into the upper cortical layers of P3 *GAD-Reelin*$^{F/F}$ mice. These neurons are expected to express Reelin 4 to 5 d later (by E17–E18) (29). Mice analyzed at P18 showed numerous grafted MGE precursors that had migrated and integrated into the host cortex, as previously described (46), as well as occasional accumulations of GFP$^+$ neurons in layer I or just above layer I. A subset of grafted neurons expressed Reelin (~25%). The density of ectopic Cux1$^+$ neurons was markedly

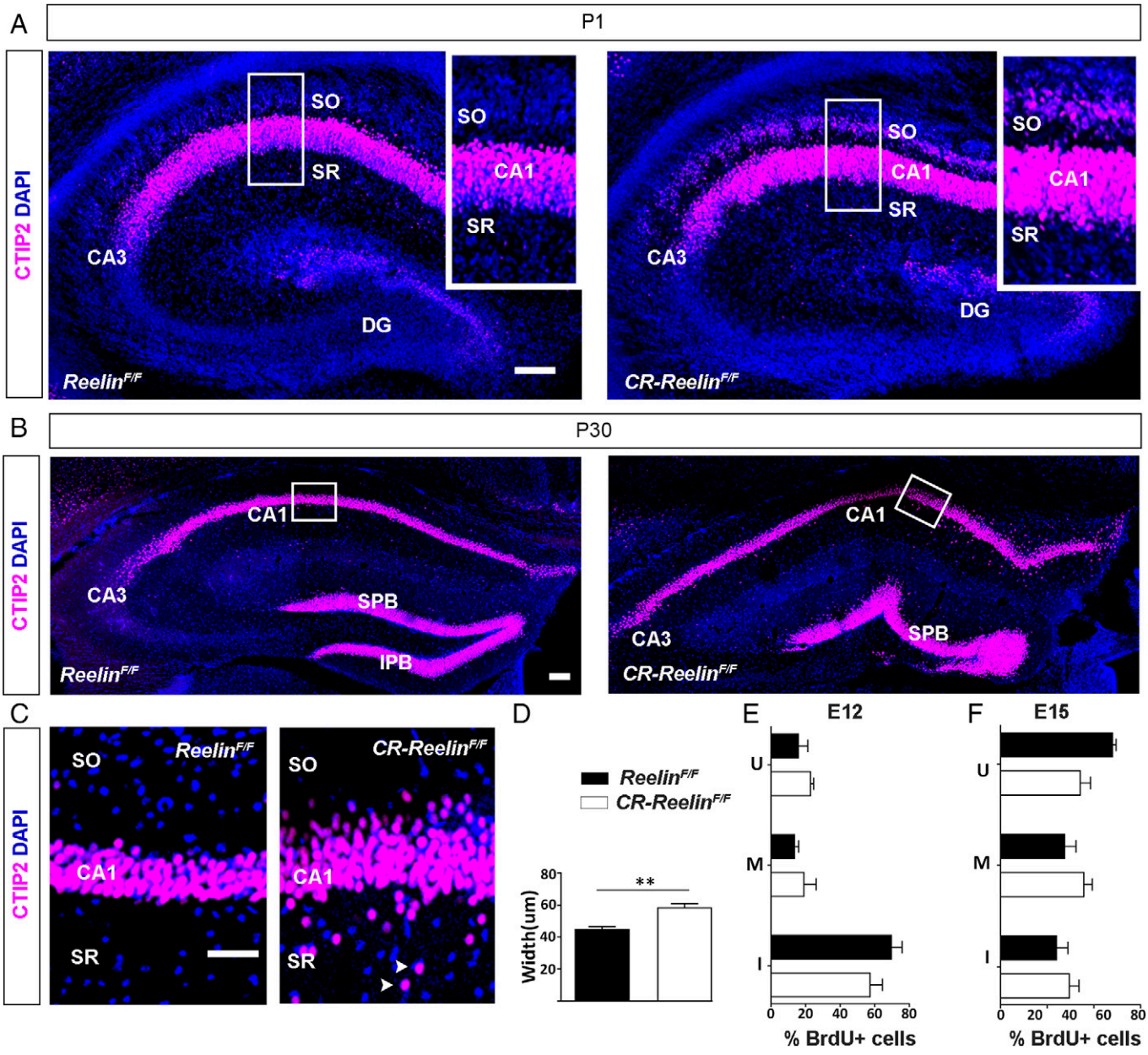

Fig. 4. CA1 cytoarchitecture in the absence of Reelin from CR cells. (*A*–*C*) Representative CTIP2 confocal images of the hippocampus CA1 at P1 (*A*) and P30 (*B* and *C*) in *Reelin*$^{F/F}$ (*Left*) and *CR-Reelin*$^{F/F}$ (*Right*) mice showing a wider cell distribution and ectopic location (arrowheads in *C*) of pyramidal cells in the SR of *CR-Reelin*$^{F/F}$ mice, which is suggestive of migration abnormalities. (*D*) Analysis of CA1 width. (*E* and *F*) Analysis of BrdU^{+} cell distribution in the CA1 of mice injected with BrdU at E12 (*E*) or E15 (*F*) show very mild alterations in the inside-out order of positioning in the *CR-Reelin*$^{F/F}$ CA1. Data represent mean ± SEM. Statistical analysis: (*D*) unpaired two-tailed Student's *t* test, t = 4.883 df = 6 $P = 0.0028$; $^{**}P < 0.01$, $n = 4$ mice per genotype. (*E*) Layer × genotype interaction $F(2, 21) = 2.205$ $P = 0.1352$, n.s.; *Reelin*$^{F/F}$ $n = 5$ and *CR-Reelin*$^{F/F}$ $n = 4$. (*F*) Layer × genotype interaction $F(2, 18) = 4.877$ $P = 0.0203$; two-way ANOVA with Bonferroni post hoc test n.s.; $n = 4$ mice per genotype. (Scale bar in *A* and *B*, 100 μm; *C*, 50 μm.) Upper layer (U), middle layer (M), inner layer (I), suprapyramidal blade (SPB), and infrapyramidal blade (IPB).

decreased just beneath the clusters of Reelin^{+}/GFP^{+} superficial neurons, in sharp contrast with neighboring cortical areas and the contralateral, control cortex (Fig. 6 *F*–*I* and *SI Appendix*, Fig. S10). These data support the notion that postnatal Reelin expression (around P7–P8 onwards) in superficial layers reduces the invasion of Cux1^{+} neurons into layer I, supporting the view that CR cells and GABAergic neurons cooperate through development.

Discussion

Reelin expression is prominent in CR cells during early stages, with these pioneer neurons disappearing by cell death at later stages, concomitant with the expression of Reelin in GABAergic interneurons located through the cortical layers, including layer I. Reelin expression in interneurons persists into adulthood. This developmental pattern has led to the assumption that while Reelin derived from CR cells is essential for neuronal migration, expression by interneurons is important for adult neural plasticity, as well as being involved in the pathological mechanisms of brain diseases. The present study aimed to identify the specific contribution of CR cell– and GABAergic cell–expressed Reelin in neuronal migration and corticogenesis.

Essential Role of CR Cell–Expressed Reelin in the Layering of the Neocortex. Our data show that the inactivation of Reelin in CR cells severely impairs neuronal migration in the neocortex.

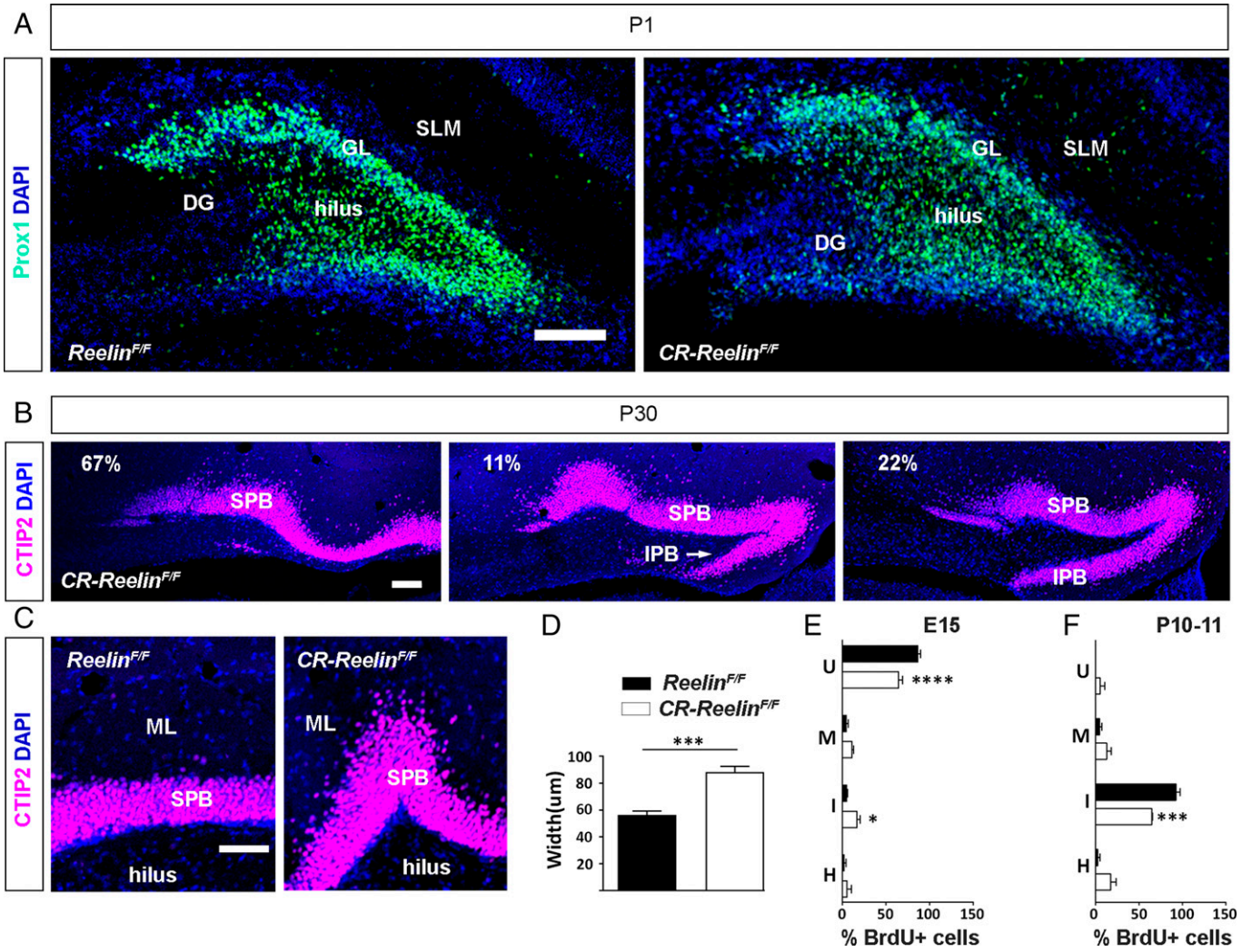

Fig. 5. Dentate gyrus phenotypes in the absence of Reelin from CR cells. (*A*) Prox1 confocal images of the hippocampus DG at P1 showing a less delineated GL in the *CR-Reelin*$^{F/F}$ DG (*Right*) compared to the *Reelin*$^{F/F}$ (*Left*). (*B*) Representative CTIP2 confocal images of the hippocampus DG at P30, depicting the different infrapyramidal blade phenotypes found in *CR-Reelin*$^{F/F}$ mice that range from complete absence or dramatically reduced IPB in the majority of cases (67% and 11%, respectively) to >350 μm IPB present (*Right*, 22%). (*C*) Suprapyramidal blade GL magnification stained with CTIP2 in *Reelin*$^{F/F}$ (*Left*) and *CR-Reelin*$^{F/F}$ mice (*Right*). (*D*) SPB GL width analysis evidencing a thicker GL in *CR-Reelin*$^{F/F}$ mice (*Right*). (*E* and *F*) Analysis of BrdU^{+} cell distribution in the SPB of the DG of mice injected with BrdU at E15 (*E*) or P10–P11 (*F*), further confirming the GC lamination abnormalities present in *CR-Reelin*$^{F/F}$ mice. Data represent mean ± SEM. Statistical analysis: (*D*) unpaired two-tailed Student's *t* test, t = 6.211 df = 6 $P = 0.0008$; ***$P < 0.001$, $n = 4$ mice per genotype. (*E*) Layer × genotype interaction $F(3, 24) = 15.65$ $P < 0.0001$; two-way ANOVA with Bonferroni post hoc test; *$P < 0.05$, ****$P < 0.0001$ $n = 4$ mice per genotype. (*F*) Layer × genotype interaction $F(3, 16) = 11.36$ $P = 0.0003$; two-way ANOVA with Bonferroni post hoc test; ***$P < 0.001$, $n = 3$ mice per genotype. (Scale bar in *A* and *B*, 100 μm; *C*, 50 μm.) Hilus (H).

Cux1^{+} layer II–III-fated neurons fail to migrate correctly to these layers and instead settle permanently in deep cortical layers. These abnormally located neurons were confirmed to be layer II–III-fated cells by BrdU-pulse studies and by in utero electroporation of GFP at E14.5. In addition, layer V–VI neurons show a wider distribution in mice lacking CR cell–derived Reelin. Because these mutants express Reelin in GABAergic interneurons throughout the cortex, we conclude that the expression of Reelin in CR cells is necessary for the correct migration and positioning of layer II–VI neurons. However, migration deficits in *CR-Reelin*$^{F/F}$ mice are considerably less dramatic than in *reeler* mutants, which exhibit an almost complete inversion of cortical layers (2, 7, 47). These data suggest that although Reelin expressed by GABAergic neurons is not sufficient to fully rescue the *reeler*-like deficits, it is likely to compensate for some of these defects, thus suggesting the cooperation between CR and GABAergic cell–derived Reelin in the migration and positioning of layer II–VI neurons. Finally, Reelin expression in a subset of subventricular zone (SVZ)/IZ cells (presumed GABAergic migrating neurons) (25, 26, 48) could also contribute to compensating the loss of CR cell–derived Reelin at prenatal stages.

Sequential Expression of Reelin in CR Cells and GABAergic Neurons Is Necessary to Prevent Ectopic Invasion of Layer I. The lack of Reelin in CR cells leads layer II–III neurons to invade the MZ/layer I at perinatal stages. This phenotype is corrected at postnatal stages, suggesting that the expression of Reelin in GABAergic neurons in layer I is sufficient to correct this ectopic location, even at late stages. This view is supported by complementary observations in which the lack of Reelin in GABAergic neurons results in the correct positioning of layer II–III neurons at perinatal stages (due to Reelin from CR cells), but in a later and permanent invasion of upper layer neurons into layer I, and by the MGE precursor grafting experiments showing that postnatal Reelin expression in GABAergic neurons markedly reduces the invasion of layer I. These data indicate not only an essential role of Reelin in preventing the aberrant invasion of layer I, but also that Reelin expression by both CR cells

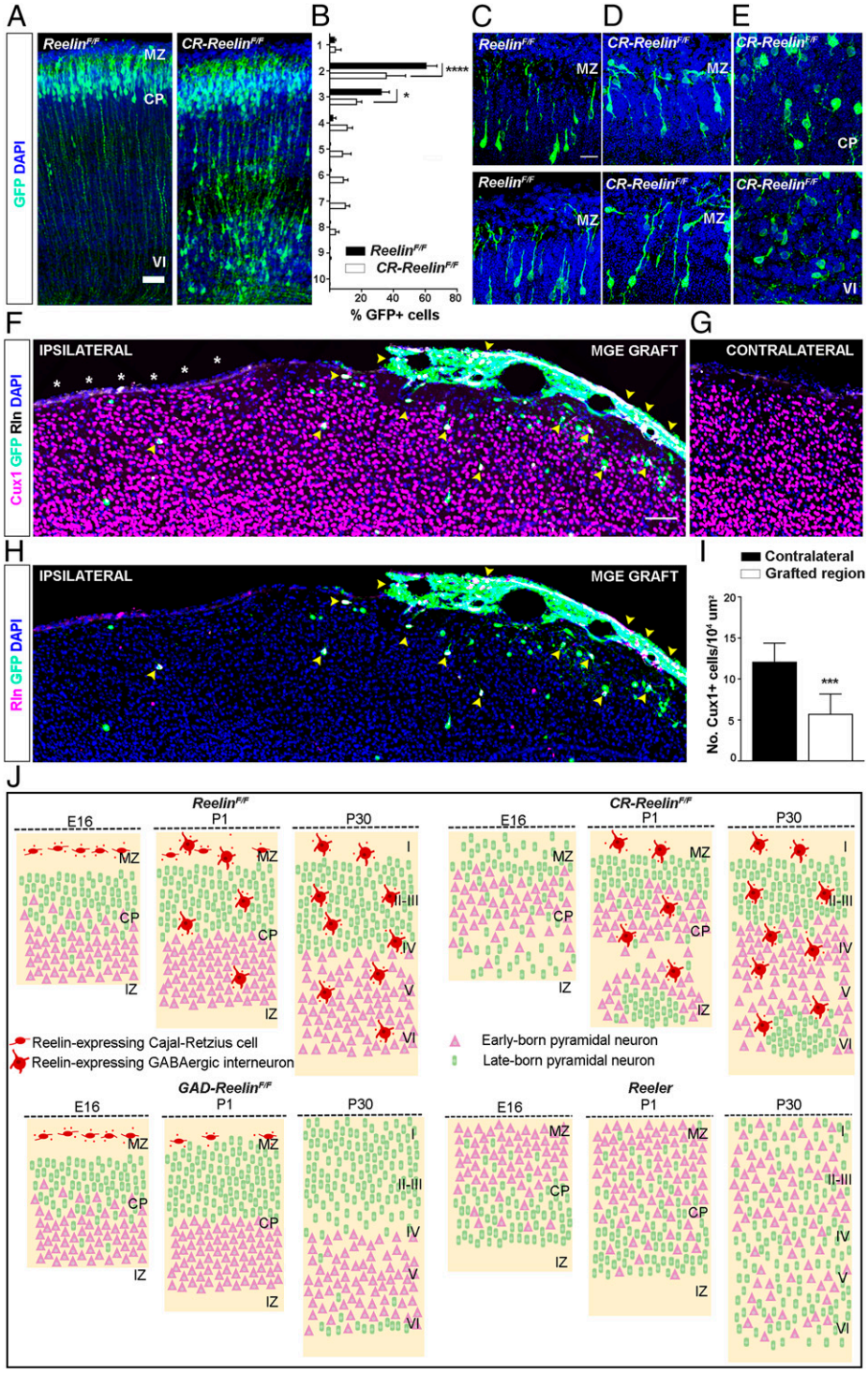

Fig. 6. Electroporation and transplantation experiments showing *reeler*-like morphological phenotypes and rescue of layer I invasion. (*A*) Confocal images of GFP staining in the cortex of P1 *Reelin*$^{F/F}$ (*Left*) and *CR-Reelin*$^{F/F}$ mice (*Right*) electroporated at E14.5. Abnormal positioning of GFP^{+} neurons is evident in *CR-Reelin*$^{F/F}$ mice. (*B*) Quantification of the percentage of GFP^{+} cells per bin at P1. (*C–E*) Confocal images of the MZ (*C*) *Reelin*$^{F/F}$ (*D*) *CR-Reelin*$^{F/F}$ mice CP (*E*, *Top*) and layer VI (*E*, *Bottom*), illustrating marked morphological alterations in *CR-Reelin*$^{F/F}$ mice. (*F–H*) Representative images of the ipsilateral (*F* and *H*) and contralateral (*G*) hemispheres of *GAD-Reelin*$^{F/F}$ mice grafted with GFP^{+} MGE cells at P3 and killed at P18. Images evidence the contrasting distribution of Cux1^{+} cells (magenta) in the MGE grafted region (green) where there are plenty of GFP^{+} cells expressing Reelin (*F* and *H*, yellow arrowheads; many in superficial layers), compared with the nongrafted ipsilateral (asterisks, *F* and *H*) and contralateral regions (*G*), where Reelin expression is low or absent, respectively. Note the decreased number of Cux1^{+} ectopic neurons in layer I of the grafted region compared to the adjacent ipsilateral (asterisk region) and the contralateral control region (*I*). (*J*) Model of Reelin functions in corticogenesis based on the data obtained from the cell-specific Reelin-deficient models. Note that in the absence of Reelin from CR cells, neuronal migration is remarkably altered and clusters of upper layer–fated neurons settle permanently in deep cortical layers. However, no permanent layer I invasion is observed and the defects are less dramatic than those found in *Reeler* mice. In contrast, in the absence of Reelin from GABAergic interneurons, a dramatic and progressive invasion of layer I by upper layer–fated neurons takes place accompanied by mild defects in the rest of the layers. These results suggest, on the one hand, that CR-derived Reelin has a critical role in the correct migration and positioning of cortical neurons and that GABAergic interneuron–derived Reelin is able to partially compensate for some of those defects. On the other hand, they suggest that sequential expression of Reelin from CR and GABAergic interneurons is essential to prevent layer I invasion. Data represent mean ± SEM. Statistical analysis: (*B*) layer × genotype interaction $F(4, 50) = 5.539$ $P < 0.0001$; two-way ANOVA with Bonferroni post hoc test *$P < 0.05$, ****$P < 0.0001$; *Reelin*$^{F/F}$ $n = 4$ and *CR-Reelin*$^{F/F}$ $n = 3$. (*I*) Paired two-tailed Student's *t* test, t = 38.96, df = 2 $P = 0.0007$; ***$P < 0.001$, $n = 3$ mice. (Scale bar in *A*, 50 μm; *C*, 20 μm; and *F*, 100 μm.)

and GABAergic interneurons acts in a cooperative and sequential manner: CR cells at early stages and GABAergic neurons at postnatal and adult stages.

The phenotypic rescue of layer I invasion observed in *CR-Reelin*$^{F/F}$ mice suggests that postmitotic neurons are able to migrate not only toward this layer but also away from it (from layer I to layers II–III). Thus, postmitotic neurons could maintain the capacity to migrate and translocate their cell bodies long after their initial settling and positioning, by mechanisms that may include inward locomotion migration, somal translocation, or multipolar migration (49). These findings may challenge current views about the dynamics of postnatal neurons, suggesting a pivotal role of Reelin in the stabilization of cortical cytoarchitecture. In addition to the ectopic location of layer II–III neurons in layer I, the lack of Reelin from GABAergic neurons led to weaker alterations in cortical layers in comparison with the lack of CR cell–derived Reelin. We thus observed small numbers of E15-generated neurons located ectopically in deep layers, and an overall wider distribution of neurons—particularly Cux1^{+} neurons—in the remaining layers. These data suggest that GABAergic neuron–derived Reelin is necessary for fine tuning the inside-out gradient of cortical neuronal migration and, especially, to prevent invasion of layer II–III neurons into layer I. Some of the present findings in adult *GAD-Reelin*$^{F/F}$ mice differ from those in a recent study using *Dlx5/6-Cre/Reelin*$^{F/F}$ mice (42), which may be attributable to the different Cre drivers and experimental approaches employed.

Reelin Expressed by CR Cells Is Necessary for the Morphogenesis and Lamination of the Hippocampus. In the hippocampus, Reelin expression by CR cells is necessary for the morphogenetic development of the infrapyramidal blade in the DG. The lack of CR cell–derived Reelin results in the absence (or dramatic reduction) of the blade. This alteration occurs despite the considerable expression of Reelin in hippocampal GABAergic neurons. This observation emphasizes the relevance of Reelin derived from CR cells for this abnormality. At early postnatal stages, CR cells located around the hippocampal fissure tangentially migrate below the pia, as the infrapyramidal blade develops (50). These migrating CR cells were not observed in *CR-Reelin*$^{F/F}$ mutants. It is thus likely that Reelin expressed by CR cells themselves is necessary for the migration of this cell population into the emerging infrapyramidal blade, thus pointing to an autologous role of CR cell–expressed Reelin.

CR-Reelin$^{F/F}$ mice exhibited additional alterations in the DG, including prominent GC invasion of the ML and Hilus, GC dispersion in the GL, and an abnormal pattern of outside-in migration within the GL. Milder phenotypes were found in the pyramidal layer, which was slightly thicker and presented a few ectopic neurons in the SR. These results suggest that, besides the lack of Reelin expression in CR cells, Reelin expressed by GABAergic neurons in the hippocampus proper is sufficient to orchestrate a nearly normal pattern of migration and lamination; in contrast, in the DG GABAergic neuron expressed Reelin is not sufficient to compensate CR cell–derived Reelin, with the latter source being necessary for the proper migration and layer distribution of GCs. As GCs are largely born postnatally, our data indicate that Reelin expressed by the large population of CR cells surviving in the postnatal/adult hippocampus is crucial for GC migration and settling throughout the entire neurogenetic period. In fact, Reelin signaling is necessary for the proper location and maturation of adult-born GCs (30, 31).

The lack of clear hippocampal phenotypes in *GAD-Reelin*$^{F/F}$ mice is likely to reflect the large numbers of CR cells surviving in this region during postnatal and adult ages (estimated to be 30% in mice) (51, 52), suggesting that Reelin expressed by CR cells is sufficient not only to orchestrate migration and lamination during development but also to maintain postnatal and adult cytoarchitectonics, particularly in the DG.

Conclusions

The present findings allow us to propose that Reelin expressed by CR cells and GABAergic neurons cooperate to orchestrate neuronal migration and corticogenesis (Fig. 6*J* and *SI Appendix*, Fig. S11). In the neocortex, Reelin expressed by CR cells in layer I largely regulates early cortical migration and the inside-out pattern of CP-fated neurons, with a fine-tuning contribution from Reelin-producing GABAergic neurons. As development progresses and CR cells are lost, this role is acquired by Reelin derived from GABAergic cells, preventing the invasion of layer I. Cooperation and compensation of these two cellular sources of Reelin is better shown in the hippocampus proper where the expression of this protein in either CR cells or GABAergic neurons alone is sufficient to allow a nearly normal hippocampal cytoarchitecture, far different from that found in *reeler* mutants. In contrast, GABAergic neurons in the DG, where most neurons are produced postnatally, are capable of compensating some, but not all, of the migratory deficits caused by the lack of Reelin in CR cells. Finally, our results point to a model of Reelin action in which, in addition to the positional and spatial signaling provided by its expression at defined sites (e.g., layer I), the extracellular diffusion of this protein or its fragments produced in distinct layers is likely to be sufficient to fulfill most Reelin functions in corticogenesis. This is well illustrated in the hippocampus proper, where the expression of Reelin in layers around the PL (stratum oriens [SO] and SR) rescues most of the migratory defects caused by the lack of Reelin expression in CR cells in the upper SLM.

Our findings may provide a better understanding of the cellular mechanisms involved in the pathogenesis of human neuropsychiatric disorders linked to abnormal neuronal migration. Some migration alterations described in schizophrenia (53), with decreased Reelin expression in cortical GABAergic neurons (54–56), are similar to the migration deficits found in *GAD-Reelin*$^{F/F}$ mice. Also, cortical alterations resembling some of the features described herein have been reported in autism, including the presence of neurons in layer I, invasion of GCs in the ML (57), and patches of disorganized cortex concomitant with reduced levels of Reelin (58). Interestingly, low expression of Reelin (59), dysfunction of the Reelin pathway (41), and also *RELN* variations and mutations (39, 60, 61) have been linked to autism spectrum disorders.

Materials and Methods

Animals. The *Mlu*I-Eco47III cloning vector (13,914 bp) was used to create a targeting vector that contained exon 1 of the Reelin sequence flanked by LoxP sites and downstream and upstream genomic sequences for homologous recombination (*SI Appendix*, Fig. S1*A*). The construct was electroporated into embryonic stem (ES) cells. Chimeric founder mice were obtained by injection of ES cells harboring the floxed Reelin allele into C57BL/6J blastocysts. Chimeras were crossed with C57BL/6J mice and the resulting offspring (heterozygous floxed Reelin mice, *Reelin*$^{F/WT}$) were backcrossed to obtain homozygous floxed Reelin mice (*Reelin*$^{F/F}$) in a C57/Bl6 background. *Reelin*$^{F/F}$ mice were crossed with cell-specific constitutive Cre recombinase mice to obtain double transgenic mice with specific deletion of the Reelin gene either in Cajal–Retzius cells [*Calb2*$^{tm1(cre)Zjh}$/J, stock #010774, The Jackson Laboratory] or GABAergic interneurons [*Gad2*$^{tm2(cre)Zjh}$/J, stock #010802, The Jackson

Laboratory] (62). Cre homozygous (*CR-Reelin*$^{F/F}$ and *GAD-Reelin*$^{F/F}$) mice and those without Cre (*Reelin*$^{F/F}$) were used for experimental purposes following the guidelines of the European Community Directive 2010/63/EU, and were approved by the Ethics Committee for Animal Experimentation of the University of Barcelona.

Tissue Processing and Immunohistochemistry. Embryonic tissue (E12, E16) was fixed by immersion in 4% paraformaldehyde (PFA); late embryos (E18–E19) and postnatal mice (P1, P15, and P30) were deeply anesthetized and transcardially perfused with 4% PFA, cryoprotected, and frozen. Sections were kept at −20 °C until use. For immunodetection, sections were blocked. For BrdU and CTIP2 detection, heat-mediated antigen retrieval was performed before blocking. Primary antibodies were incubated overnight at 4 °C. Sections were incubated for 2 h at room temperature with Alexa Fluor secondary antibodies (1:500) and then counterstained with Hoechst. Sections were then mounted in Mowiol.

Western Blot. The cortex and hippocampus of each hemisphere were dissected, frozen in liquid nitrogen, and stored at −80 °C until use. Brain tissue was processed as previously described (30). After incubation with antibodies, membranes were developed with the Enhanced Chemiluminescence (ECL) system.

BrdU Administration. Pregnant females from timed mating crossings were given two pulses of BrdU (50 mg/kg; 2-h interval between injections) at E12 and E15 to label the lower and upper cortical layer cells, respectively. The resulting offspring were killed at P30. For postnatal administration, pups were injected with BrdU (50 mg/kg) at P10 and P11 and were killed at P30. Tissue was collected for immunohistochemistry as previously described.

Electroporation. Mouse embryos were electroporated in utero at E14.5 as previously described (63). Electroporated embryos (E18–E19) and P1 pups were perfused with 4% PFA and processed for GFP immunostaining.

Transplantation Experiments. MGE transplantations were done as described (46). E13.5 C57BL/6J/GFP^{+} (64) embryos were placed in Dulbecco's Modified Eagle's Medium/Nutrient Mixture F-12 Ham (DMEM/F12) medium (GIBCO), and the ventricular and subventricular zones of the anterior part of the MGE were dissected as described (65, 66). Tissue explants were collected in DMEM/F12 medium and dissociated. The cells were pelleted by centrifugation and resuspended in DMEM/F12 medium. MGE cell suspensions were front loaded into beveled glass micropipettes. P3 mice were anesthetized by hypothermia. A microinjector and stereotaxic frame were used to deliver a total of 2×10^5 MGE cells per mouse distributed unilaterally across four cortical points (50 to 100 nL per site) through two injection sites corresponding to the somatosensory cortex. At P18 mice were perfused and processed for immunohistochemistry.

Image Acquisition and Data Analysis. Bright-field images were acquired with an Olympus D72 camera attached to a Nikon Eclipse E600 microscope and with a NanoZoomer 2.0-HT (Hamamatsu Photonics). Fluorescent images were taken using a Leica TCS SP5 confocal microscope, a Nikon Eclipse E600 microscope (BrdU images), a NanoZoomer 2.0-HT, and a Leica Thunder DMi8 microscope attached to a Leica K5, SCMOS camera. Image processing was done with FIJI (ImageJ). To determine the layer distribution of cells in the cortex (Cux1 for upper layers, CTIP2 for lower layers, BrdU, and GFP), images from the primary somatosensory barrel field (SBF1) were taken using 10×, 20×, and 40× oil-immersion objectives on a Leica TCS SP5 confocal microscope. Cortical strips were divided into 10 identical bins of 70 μm width using a macro created in ImageJ (FIJI), and the number of cells in each bin was counted manually. To analyze the distribution of BrdU^{+} cells in the granule cell layer of the DG (BrdU at E15 and P10–P11) and the CA1 (BrdU at E12 and E15), the cell layers were subdivided into three layers (upper, middle, and inner) and the number of BrdU^{+} cells in each position was counted. In the DG, the number of BrdU^{+} cells located in the hilus was also counted. The thickness of the layered hippocampal structures CA1 and DG was determined by measuring the average width of each structure.

Statistical Analysis. All statistical analyses were performed using GraphPad Prism 6.0 software (GraphPad Software, Inc). Data were analyzed using either the two-tailed unpaired *t* test or two-way Analysis of Variance (ANOVA) with multiple comparison post hoc tests, unless otherwise stated. Statistical significance was established at $P \leq 0.05$.

Data, Materials, and Software Availability. All study data are included in the article and/or supporting information. Genetically modified mice will be made available upon reasonable request.

ACKNOWLEDGMENTS. Parts of this manuscript are based on Alba Vílchez-Acosta's PhD thesis (https://www.tdx.cat/handle/10803/668316#page=1). We thank Nuria Masachs, Carles Bosch, and Ashraf Muhaisen for help in the management of mouse colonies; Manel Bosch from the Centros Científicos y Tecnológicos de la Universitat de Barcelona for his assistance in image analysis; and Sara E. Rubio for English editing. This work was supported by grants from the Spanish Ministerio de Ciencia y Competitividad and Ministerio de Ciencia e Innovación (SAF2016-76340R and PID2019-106764RB-C21, Excellence Unit 629, María de Maeztu/Institute of Neurosciences) and by Centro de Investigación Biomédica en Red de Enfermedades Neurodegenerativas (Instituto de Salud Carlos III, Spanish Ministry of Health) (to E.S.).

Author affiliations: [a]Department of Cell Biology, Physiology, and Immunology, Faculty of Biology, Institute of Neurosciences, Universitat de Barcelona, 08028 Barcelona, Spain; [b]Centro de Investigación Biomédica en Red Enfermedades Neurodegenerativas, Instituto de Salud Carlos III, Madrid, 28031 Spain; [c]Instituto de Neurociencias, Consejo Superior de Investigaciones Científicas and Universidad Miguel Hernández, 03550 Sant Joan d'Alacant, Spain; [d]Department of Experimental Psychology, Universidad de Sevilla, 41018 Sevilla, Spain; [e]Andalusian Center for Molecular Biology and Regenerative Medicine, Consejo Superior de Investigaciones Científicas, Seville 41092, Spain; and [f]Department of Psychiatry, Yale University School of Medicine, New Haven, CT 06508 United States of America

1. O. Marín, Interneuron dysfunction in psychiatric disorders. *Nat. Rev. Neurosci.* **13**, 107–120 (2012).
2. G. D'Arcangelo *et al.*, A protein related to extracellular matrix proteins deleted in the mouse mutant reeler. *Nature* **374**, 719–723 (1995).
3. D. S. Rice, T. Curran, Role of the Reelin signaling pathway in central nervous system development. *Annu. Rev. Neurosci.* **24**, 1005–1039 (2001).
4. J. A. Cooper, A mechanism for inside-out lamination in the neocortex. *Trends Neurosci.* **31**, 113–119 (2008).
5. F. Tissir, A. M. Goffinet, Reelin and brain development. *Nat. Rev. Neurosci.* **4**, 496–505 (2003).
6. T. Miyata, K. Nakajima, K. Mikoshiba, M. Ogawa, Regulation of Purkinje cell alignment by Reelin as revealed with CR-50 antibody. *J. Neurosci.* **17**, 3599–3609 (1997).
7. M. Ogawa *et al.*, The reeler gene-associated antigen on Cajal-Retzius neurons is a crucial molecule for laminar organization of cortical neurons. *Neuron* **14**, 899–912 (1995).
8. M. Trommsdorff *et al.*, Reeler/disabled-like disruption of neuronal migration in knockout mice lacking the VLDL receptor and ApoE receptor 2. *Cell* **97**, 689–701 (1999).
9. B. W. Howell, R. Hawkes, P. Soriano, J. A. Cooper, Neuronal position in the developing brain is regulated by mouse disabled-1. *Nature* **389**, 733–737 (1997).
10. M. Sheldon *et al.*, Scrambler and yotari disrupt the disabled gene and produce a reeler-like phenotype in mice. *Nature* **389**, 730–733 (1997).
11. S. Simó, J. A. Cooper, Rbx2 regulates neuronal migration through different cullin 5-RING ligase adaptors. *Dev. Cell* **27**, 399–411 (2013).
12. M. Segarra *et al.*, Endothelial Dab1 signaling orchestrates neuro-glia-vessel communication in the central nervous system. *Science* **361**, eaao2861 (2018).
13. M. Marín-Padilla, Cajal-Retzius cells and the development of the neocortex. *Trends Neurosci.* **21**, 64–71 (1998).
14. E. Soriano, J. A. Del Río, The cells of Cajal-Retzius: Still a mystery one century after. *Neuron* **46**, 389–394 (2005).
15. V. Borrell, O. Marín, Meninges control tangential migration of hem-derived Cajal-Retzius cells via CXCL12/CXCR4 signaling. *Nat. Neurosci.* **9**, 1284–1293 (2006).
16. A. Sentürk, S. Pfennig, A. Weiss, K. Burk, A. Acker-Palmer, Ephrin Bs are essential components of the Reelin pathway to regulate neuronal migration. *Nature* **472**, 356–360 (2011).
17. Y. Jossin, J. A. Cooper, Reelin, Rap1 and N-cadherin orient the migration of multipolar neurons in the developing neocortex. *Nat. Neurosci.* **14**, 697–703 (2011).
18. X. Chai, E. Förster, S. Zhao, H. H. Bock, M. Frotscher, Reelin stabilizes the actin cytoskeleton of neuronal processes by inducing n-cofilin phosphorylation at serine3. *J. Neurosci.* **29**, 288–299 (2009).
19. Y. Matsunaga *et al.*, Reelin transiently promotes N-cadherin-dependent neuronal adhesion during mouse cortical development. *Proc. Natl. Acad. Sci. U.S.A.* **114**, 2048–2053 (2017).
20. C. Gil-Sanz *et al.*, Cajal-Retzius cells instruct neuronal migration by coincidence signaling between secreted and contact-dependent guidance cues. *Neuron* **79**, 461–477 (2013).
21. K. Hashimoto-Torii *et al.*, Interaction between Reelin and Notch signaling regulates neuronal migration in the cerebral cortex. *Neuron* **60**, 273–284 (2008).
22. K. Sekine *et al.*, Reelin controls neuronal positioning by promoting cell-matrix adhesion via inside-out activation of integrin α5β1. *Neuron* **76**, 353–369 (2012).
23. K. Kubo *et al.*, Ectopic Reelin induces neuronal aggregation with a normal birthdate-dependent "inside-out" alignment in the developing neocortex. *J. Neurosci.* **30**, 10953–10966 (2010).
24. L. Dulabon *et al.*, Reelin binds alpha3beta1 integrin and inhibits neuronal migration. *Neuron* **27**, 33–44 (2000).
25. Y. Hirota, K. Nakajima, Control of neuronal migration and aggregation by Reelin signaling in the developing cerebral cortex. *Front. Cell Dev. Biol.* **5**, 40 (2017).

26. M. Yoshida, S. Assimacopoulos, K. R. Jones, E. A. Grove, Massive loss of Cajal-Retzius cells does not disrupt neocortical layer order. *Development* **133**, 537–545 (2006).
27. C. A. de Frutos *et al.*, Reallocation of olfactory Cajal-Retzius cells shapes neocortex architecture. *Neuron* **92**, 435–448 (2016).
28. H. Supèr, J. A. Del Río, A. Martínez, P. Pérez-Sust, E. Soriano, Disruption of neuronal migration and radial glia in the developing cerebral cortex following ablation of Cajal-Retzius cells. *Cereb. Cortex* **10**, 602–613 (2000).
29. S. Alcántara *et al.*, Regional and cellular patterns of Reelin mRNA expression in the forebrain of the developing and adult mouse. *J. Neurosci.* **18**, 7779–7799 (1998).
30. L. Pujadas *et al.*, Reelin regulates postnatal neurogenesis and enhances spine hypertrophy and long-term potentiation. *J. Neurosci.* **30**, 4636–4649 (2010).
31. C. M. Teixeira *et al.*, Cell-autonomous inactivation of the Reelin pathway impairs adult neurogenesis in the hippocampus. *J. Neurosci.* **32**, 12051–12065 (2012).
32. L. Groc *et al.*, NMDA receptor surface trafficking and synaptic subunit composition are developmentally regulated by the extracellular matrix protein Reelin. *J. Neurosci.* **27**, 10165–10175 (2007).
33. U. Beffert *et al.*, Modulation of synaptic plasticity and memory by Reelin involves differential splicing of the lipoprotein receptor Apoer2. *Neuron* **47**, 567–579 (2005).
34. S. E. Hong *et al.*, Autosomal recessive lissencephaly with cerebellar hypoplasia is associated with human RELN mutations. *Nat. Genet.* **26**, 93–96 (2000).
35. I. Knuesel *et al.*, Maternal immune activation and abnormal brain development across CNS disorders. *Nat. Rev. Neurol.* **10**, 643–660 (2014).
36. E. Dazzo *et al.*, Heterozygous Reelin mutations cause autosomal-dominant lateral temporal epilepsy. *Am. J. Hum. Genet.* **96**, 992–1000 (2015).
37. F. Impagnatiello *et al.*, A decrease of Reelin expression as a putative vulnerability factor in schizophrenia. *Proc. Natl. Acad. Sci. U.S.A.* **95**, 15718–15723 (1998).
38. D. R. Grayson *et al.*, Reelin promoter hypermethylation in schizophrenia. *Proc. Natl. Acad. Sci. U.S.A.* **102**, 9341–9346 (2005).
39. D. B. Lammert, B. W. Howell, RELN mutations in autism spectrum disorder. *Front. Cell. Neurosci.* **10**, 84 (2016).
40. S. H. Fatemi *et al.*, Reelin signaling is impaired in autism. *Biol. Psychiatry* **57**, 777–787 (2005).
41. S. T. Baek *et al.*, An AKT3-FOXG1-Reelin network underlies defective migration in human focal malformations of cortical development. *Nat. Med.* **21**, 1445–1454 (2015).
42. J. Pahle *et al.*, Selective inactivation of Reelin in inhibitory interneurons leads to subtle changes in the dentate gyrus but leaves cortical layering and behavior unaffected. *Cereb. Cortex* **30**, 1688–1707 (2020).
43. T. Pohlkamp *et al.*, Characterization and distribution of Reelin-positive interneuron subtypes in the rat barrel cortex. *Cereb. Cortex* **24**, 3046–3058 (2014).
44. J. A. Del Río *et al.*, Differential survival of Cajal-Retzius cells in organotypic cultures of hippocampus and neocortex. *J. Neurosci.* **16**, 6896–6907 (1996).
45. S. J. Franco, I. Martinez-Garay, C. Gil-Sanz, S. R. Harkins-Perry, U. Müller, Reelin regulates cadherin function via Dab1/Rap1 to control neuronal migration and lamination in the neocortex. *Neuron* **69**, 482–497 (2011).
46. M. Martinez-Losa *et al.*, Nav1.1-overexpressing interneuron transplants restore brain rhythms and cognition in a mouse model of Alzheimer's disease. *Neuron* **98**, 75–89.e5 (2018).
47. M. P. Boyle *et al.*, Cell-type-specific consequences of Reelin deficiency in the mouse neocortex, hippocampus, and amygdala. *J. Comp. Neurol.* **519**, 2061–2089 (2011).
48. T. Uchida *et al.*, Downregulation of functional Reelin receptors in projection neurons implies that primary Reelin action occurs at early/premigratory stages. *J. Neurosci.* **29**, 10653–10662 (2009).
49. H. Tabata, K. Nakajima, Multipolar migration: The third mode of radial neuronal migration in the developing cerebral cortex. *J. Neurosci.* **23**, 9996–10001 (2003).
50. E. Förster, S. Zhao, M. Frotscher, Laminating the hippocampus. *Nat. Rev. Neurosci.* **7**, 259–267 (2006).
51. M. Anstötz *et al.*, Developmental Profile, Morphology, and Synaptic Connectivity of Cajal-Retzius Cells in the Postnatal Mouse Hippocampus. *Cereb. Cortex* **26**, 855–872 (2016).
52. J. A. del Río, A. Martínez, M. Fonseca, C. Auladell, E. Soriano, Glutamate-like immunoreactivity and fate of Cajal-Retzius cells in the murine cortex as identified with calretinin antibody. *Cereb. Cortex* **5**, 13–21 (1995).
53. S. Akbarian *et al.*, Altered distribution of nicotinamide-adenine dinucleotide phosphate-diaphorase cells in frontal lobe of schizophrenics implies disturbances of cortical development. *Arch. Gen. Psychiatry* **50**, 169–177 (1993).
54. W. B. Ruzicka *et al.*, Selective epigenetic alteration of layer I GABAergic neurons isolated from prefrontal cortex of schizophrenia patients using laser-assisted microdissection. *Mol. Psychiatry* **12**, 385–397 (2007).
55. M. B. Knable, B. M. Barci, M. J. Webster, J. Meador-Woodruff, E. F. Torrey; Stanley Neuropathology Consortium, Molecular abnormalities of the hippocampus in severe psychiatric illness: Postmortem findings from the Stanley Neuropathology Consortium. *Mol. Psychiatry* **9**, 609–620, 544 (2004).
56. S. H. Fatemi, J. A. Earle, T. McMenomy, Reduction in Reelin immunoreactivity in hippocampus of subjects with schizophrenia, bipolar disorder and major depression. *Mol. Psychiatry* **5**, 654–663, 571 (2000).
57. J. Wegiel *et al.*, The neuropathology of autism: Defects of neurogenesis and neuronal migration, and dysplastic changes. *Acta Neuropathol.* **119**, 755–770 (2010).
58. R. Stoner *et al.*, Patches of disorganization in the neocortex of children with autism. *N. Engl. J. Med.* **370**, 1209–1219 (2014).
59. S. H. Fatemi, The role of Reelin in pathology of autism. *Mol. Psychiatry* **7**, 919–920 (2002).
60. S. De Rubeis *et al.*; DDD Study; Homozygosity Mapping Collaborative for Autism; UK10K Consortium, Synaptic, transcriptional and chromatin genes disrupted in autism. *Nature* **515**, 209–215 (2014).
61. R. E. Rodin *et al.*, The landscape of mutational mosaicism in autistic and normal human cerebral cortex. bioRxiv [Preprint]. https://www.biorxiv.org/content/10.1101/2020.02.11.944413v1.full. Accessed 25 August 2022.
62. H. Taniguchi *et al.*, A resource of Cre driver lines for genetic targeting of GABAergic neurons in cerebral cortex. *Neuron* **71**, 995–1013 (2011).
63. A. Cárdenas *et al.*, Evolution of cortical neurogenesis in amniotes controlled by robo signaling levels. *Cell* **174**, 590–606.e21 (2018).
64. A. K. Hadjantonakis, M. Gertsenstein, M. Ikawa, M. Okabe, A. Nagy, Generating green fluorescent mice by germline transmission of green fluorescent ES cells. *Mech. Dev.* **76**, 79–90 (1998).
65. I. Zipancic, M. E. Calcagnotto, M. Piquer-Gil, L. E. Mello, M. Alvarez-Dolado, Transplant of GABAergic precursors restores hippocampal inhibitory function in a mouse model of seizure susceptibility. *Cell Transplant.* **19**, 549–564 (2010).
66. M. Alvarez-Dolado *et al.*, Cortical inhibition modified by embryonic neural precursors grafted into the postnatal brain. *J. Neurosci.* **26**, 7380–7389 (2006).